SAND2020-9953J

Starting point independent quantum Monte Carlo calculations of iron oxide

Joshua P. Townsend,[1,*] Sergio D. Pineda Flores,[2] Raymond C. Clay III,[1] Thomas R. Mattsson,[1] Eric Neuscamman,[2] Luning Zhao,[3] R. E. Cohen,[4] and Luke Shulenburger[1]

[1]*High Energy Density Physics Theory, Sandia National Laboratories, Albuquerque, NM 87185*

[2]*Department of Chemistry, University of California, Berkeley, CA, 94720*

[3]*Department of Chemistry, University of Washington, Seattle, WA, 98195*

[4]*Extreme Materials Initiative, Geophysical Laboratory, Carnegie Institution for Science, Washington, DC 20015-1305, USA*

Abstract

Quantum Monte Carlo (QMC) methods are useful for studies of strongly correlated materials because they are many-body in nature and use the physical Hamiltonian. Typical calculations assume as a starting point a wave function constructed from single particle orbitals (SPOs) obtained from one-body methods e.g. density functional theory. However, mean-field-derived wave functions can sometimes lead to systematic QMC biases if the mean-field result poorly describes the true ground state. Here, we study the accuracy and flexibility of QMC trial wave functions using variational and fixed-node diffusion QMC estimates of the total spin density and lattice distortion of antiferromagnetic iron oxide (FeO) in the ground state B1 crystal structure. We found that for relatively simple wave functions the predicted lattice distortion was controlled by the choice of single particle orbitals used to construct the wave function, rather than by subsequent wave function optimization techniques within QMC. We then demonstrate starting point independence of the trial wave function with respect to the energy, spin density, and predicted lattice distortion by eliminating bias via orbital optimization. The results suggest that orbital optimization is a promising method for accurate many-body calculations of strongly correlated condensed phases.

INTRODUCTION

Iron oxide (FeO) is a prototypical Mott-type insulator which displays a rich phase diagram that includes magnetic, electronic, and structural phase transformations due in part to the open shell configuration of the $3d$ electrons [1–8]. In the ground state, FeO adopts a bulk antiferromagnetic (AFM) structure composed of alternating ferromagnetic planes of Fe atoms perpendicular to [111], which induces, by magnetoelastic coupling, a symmetry lowering distortion of the nominally B1 lattice from cubic to rhombohedral [9, 10]. Previous theoretical studies have investigated structural phase transitions at high pressure and the equilibrium lattice distortion [8, 11–18]. One of the main findings of these studies is that the equilibrium lattice distortion in particular is highly sensitive to the electronic structure.

Quantum Monte Carlo (QMC) methods are especially well suited to problems where electronic correlation is important because they use the physical Hamiltonian and are therefore variational [19, 20]. The input for a typical QMC calculation is a trial wave function, the antisymmetric portion of which is often generated from a set of single particle orbitals (SPOs) from e.g. Kohn-Sham density functional theory (DFT). In addition to the antisymmetric piece, the trial wave function typically includes many adjustable parameters which can be optimized by exploiting the variational principle using, for example, variational Monte Carlo (VMC). Classic examples include the Jastrow factor, backflow transformation of the electronic coordinates, a multi-determinant expansion, or orbital optimization. Each of the above explicitly introduces electron-electron correlation into the wave function and thereby gives improved ground state properties as compared to a Hartree-Fock wave function [21–24].

The accuracy of projector-based QMC methods such as diffusion Monte Carlo (DMC) depend on the nodal surface of the wave function, which depends on the SPO set. The challenge for QMC studies of strongly correlated systems, then, lies in constructing a suitably flexible and accurate wave function. Thus new methods for generating accurate QMC trial wave functions with sufficient flexibility are highly desired. Recently, several studies have demonstrated remarkable success in constructing flexible and accurate wave functions in molecular systems[25–27], but until now wave functions for condensed systems tend to be much simpler due to the larger number of electrons and larger basis sets.

Here we report variational and diffusion quantum Monte Carlo calculations of AFM FeO using a variety of trial wave function ansätze including electron-electron backflow transfor-

mations as well as multi-determinant expansions and orbital optimization. In order to test the flexibility of the trial wave function, we constructed sets of SPOs from DFT using PBE and PBE+U functionals generated so as to yield qualitatively different lattice distortions. We then demonstrate starting point independence of DMC estimates of the energy, spin density, and equilibrium lattice distortion with respect to the SPOs in a Slater Jastrow wave function through orbital optimization. The results indicate that orbital optimization is a promising method for constructing very accurate and flexible wave functions for QMC calculations on challenging transition metal oxides and highlight the ability of QMC methods to deliver starting point independent estimates of some ground state properties.

COMPUTATIONAL APPROACH

The immediate goal of this study was to understand how the techniques used to construct QMC trial wave functions affected the estimated ground state properties in a challenging condensed system. With that goal in mind, we restricted calculations to a single four-atom AFM primitive cell [28] with periodic boundary conditions so that advanced wave function ansätze which scale unfavorably with system size could be tested.

The building block of all the trial wave functions considered here was the Slater-Jastrow (SJ) type wave function:

$$\Psi_T(\mathbf{r};\xi) = D^{\uparrow}(\mathbf{x};\xi)D^{\downarrow}(\mathbf{x};\xi)e^{J(\mathbf{x};\xi)} \tag{1}$$

where $\mathbf{r}$,$\mathbf{x}$ are the sets of electronic and generalized coordinates, respectively, ξ is the set of variational parameters, and $D^{\uparrow,\downarrow}$ is a linear combination of one or more Slater determinants composed of single particle orbitals (SPOs). The adjustable parameters of the antisymmetric portion of the wave function include, for example, weights in a multi-determinant expansion, electron-electron backflow transformation, or orbital rotations. Finally, $J(\mathbf{x};\xi)$ is the Jastrow function that explicitly introduces dynamic correlation into the wave function and enforces the cusp conditions [21, 29, 30].

Projector-based QMC methods like DMC for fermions commonly require that the nodal surface ($\Psi_T(\mathbf{r};\xi) = 0$) of the trial wave function is prescribed in order to mitigate the fermion sign-problem [31]. This fixed-node (FN) approximation introduces a systematic bias in the results, which while variational, may be significant if the nodal surface of the trial wave

function is qualitatively different from that of the exact ground state wave function. As we show here, this bias can result in qualitatively incorrect behavior even after the application of projector-based QMC methods. Crucially, the Jastrow factor does not affect the nodal surface of the trial wave functions we investigated, so the ultimate accuracy of our DMC calculations is set by the anti-symmetric piece of the wave function.

Wave function generation

In order to test the flexibility of QMC trial wave functions we constructed two sets of SPOs which produced qualitatively different estimates of the spin density and equilibrium lattice distortion. Trial wave functions were constructed from SPOs generated from spin-resolved DFT calculations using the `Quantum ESPRESSO` code (version 6.4.0), an implementation of plane wave based Kohn-Sham density functional theory with periodic boundary conditions [32]. We used pseudopotentials specifically designed for QMC calculations to describe the iron and oxygen atoms for both the DFT and QMC calculations [33]. The iron pseudopotential had a neon core ($3s^2 3p^6 3d^6 4s^2$ valence) and the oxygen pseudopotential had a helium core ($2s^2 2p^4$ valence), for a total of 44 electrons in the primitive cell. All DFT calculations used a 180 Ha plane wave cutoff and a $6 \times 6 \times 6$ k-point grid and were tested to confirm that further increasing those values did not appreciably change the DFT energy or stress. The first SPO set was constructed using the PBE generalized gradient approximation [34], and the second used a PBE+U functional ($U = 4.3$ eV) in the rotationally invariant scheme following previous work[16, 17] in order to localize the Fe $3d$ states. The two sets of SPOs are qualitatively distinct. The PBE result predicted a metallic ground state and a positive lattice distortion, while the PBE+U results predicted an insulating ground state and negative lattice distortion.

Wave function optimization and Monte Carlo calculations

All QMC calculations were performed with the `QMCPACK` code (version 3.6) [35]. We used the improved adaptive shift algorithm [36] to optimize, in some cases, more than three thousand wave function parameters using variational Monte Carlo (VMC). Common amongst all trial wave functions we considered were species dependent one-, two-, and three-

body Jastrow factors represented as cubic polynomials in the particle separations with a spatial cutoff corresponding to the Wigner-Seitz radius of the cell, about 2.9 bohr. The two-body Jastrow produced the largest energy and variance reduction, but addition of one- and three-body terms was found to further reduce the energy and variance significantly. The use of small core pseudopotentials resulted in a highly oscillatory wave function near the atomic cores which was costly in terms of memory to accurately represent on a rectangular mesh. We therefore chose to divide the representation of the wave function into two parts as suggested by Esler et al. [37] with the regions near the ions stored as radial splines multiplied by spherical harmonics and the interstitial regions represented by 3D b-splines on a rectilinear mesh[38]. This scheme reduced the memory required to represent the wave function by a factor of more than 25 as compared to the standard rectangular mesh with no statistically significant change in the energy or variance.

With two sets of SPOs in hand, we proceeded to optimize the trial wave functions using VMC. While optimization of the Jastrow factor yielded significant energy and variance reduction, the SPO's themselves are what limit the ultimate accuracy of DMC. We therefore explored three methods of improving the nodal surface of the trial wave function: backflow transformation of the electronic coordinates, multi-determinant expansion, and orbital optimization. A backflow (BF) transformation is a transformation of the electronic coordinates $\mathbf{r}$, to quasiparticle coordinates $\mathbf{q}$ [39]. For a particular electron this transformation is given by:

$$\mathbf{r}_i \rightarrow \mathbf{q}_i = \mathbf{r}_i + \sum_{i \neq j} \eta(|\mathbf{r}_i - \mathbf{r}_j|; \xi)(\mathbf{r}_i - \mathbf{r}_j) \tag{2}$$

with η a spherically symmetric spline function.

The second trial wave function type was a multi-determinant (MD) expansion. In this wave function, one builds out of a set of single particle orbitals, $\{\phi\}$, a number of Slater determinants $\{\Phi[\phi]\}$, with the former being larger than the number of electrons per spin channel:

$$D(\mathbf{r}, \xi) = \sum_i \xi_i \Phi_i[\phi(\mathbf{r})] \tag{3}$$

The appeal of this ansatz is that with an infinite number of ϕ's and Φ's, this wave function is exact. The downside is that it scales exponentially in the number of particles. For that reason, we explored the use of modest multi-determinant expansions which were constructed in a two-step procedure. The first step was an optimization of the 924 determinant weights in

an expansion consisting of all possible single excitations within a basis of 64 SPOs. The second step was an optimization of all possible single and double excitations generated from the highest weighted 32 determinants from the previous step, which totaled 452 determinants. For these wave functions we found that optimization of the weights of the determinants at each twist further reduced the VMC energy by approximately 20 mHa/FeO as compared to optimization at a single twist only, due to differences in band ordering.

The third trial wave function type included an optimization of the SPOs (OO) themselves. With this method, each optimized SPO, $\tilde{\phi}$, present in the determinant is constructed from a unitary transformation of the original SPOs, ϕ [24]:

$$\tilde{\phi}_i = \sum_j \xi_{ij} \phi_j \tag{4}$$

This wave function contained over 3000 optimizable parameters, and was therefore expected to be the most flexible and accurate trial wave function type we considered.

The twist-averaged total energies for all optimized trial wave functions is shown in fig. 1. As expected, the VMC energies of the optimized backflow, multi-determinant, and orbital optimization wave functions were lower than their simpler Slater Jastrow wave function counterparts. An unexpected result was that improvements in the multi-determinant trial wave function predicted by VMC did not carry over to DMC in all cases. We attribute this result to the relatively small active space in which that wave function was constructed, and it highlights that our VMC optimization strategy improves the overall shape of the wave function, but not necessarily its nodal surface. Importantly, the DMC energies of the orbital optimized trial wave function were statistically identical regardless of the SPO set in which the optimization occurred. This striking result suggests starting-point independence of the optimized trial wave function with respect to the SPOs and was not achieved with any other wave function. Especially encouraging was that the OO wave function was much less expensive to evaluate as compared to the MD or BF, which were 2.2x and 1.6x times as expensive to evaluate as compared to the OO wave function, respectively.

After optimization, production DMC calculations were carried out on all optimized trial wave functions on a $3 \times 3 \times 3$ grid of twist vectors and the results were subsequently twist-averaged. DMC results were linearly extrapolated to zero timestep from a series of calculations with finite time steps of τ=0.01, 0.005, and 0.0025 Ha^{-1}.

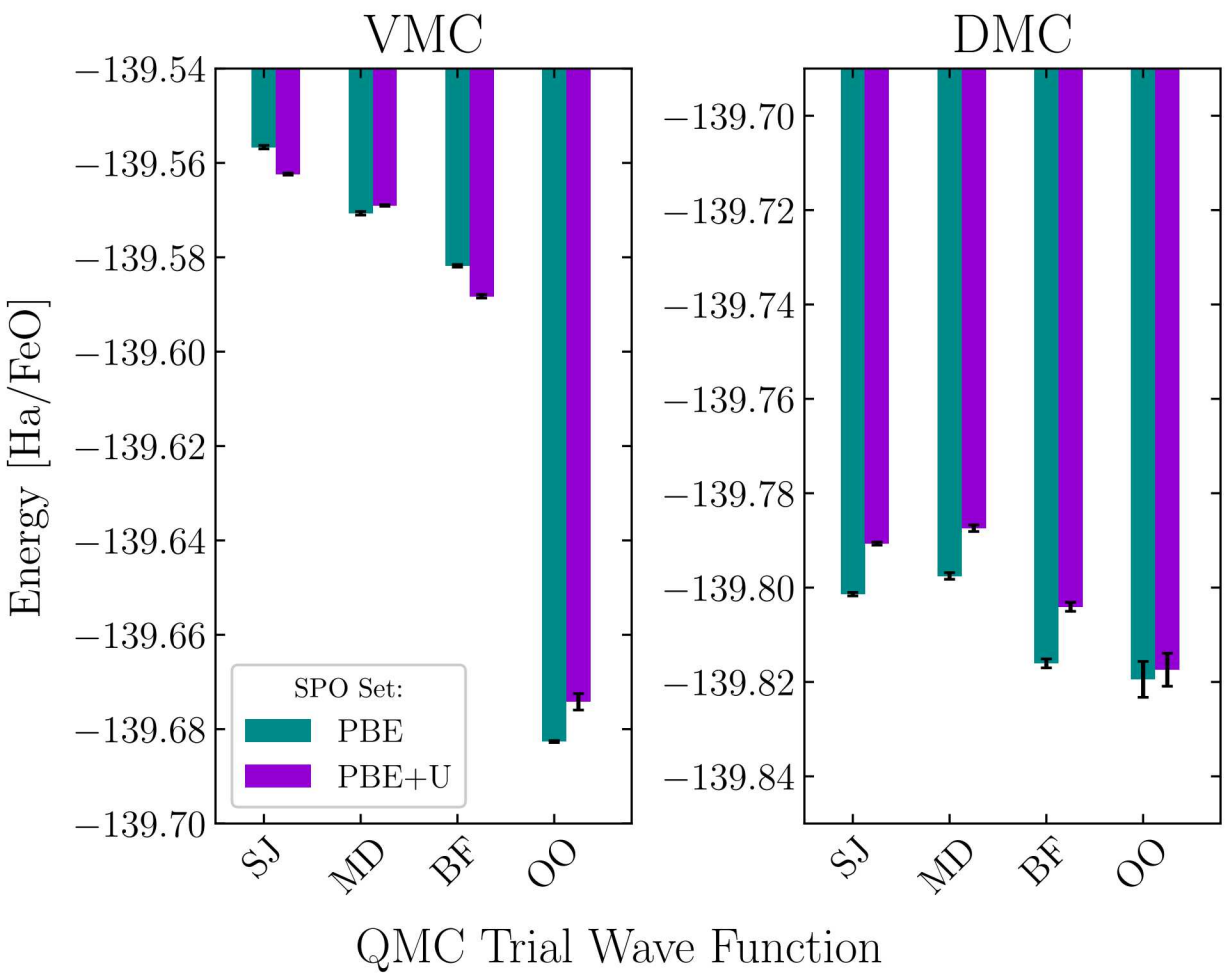

FIG. 1. (color online) Twist-averaged QMC energies for several optimized trial wave function types built from either PBE, or PBE+U SPOs. The DMC energies are linearly extrapolated to zero timestep.

RESULTS

The principal goal of this study was to understand how sensitive various ground state properties of a system were to the trial wave function for a realistic and challenging condensed system. To that end, we calculated a series of physical properties that are typically strongly affected by the electronic structure: the total spin density and the equilibrium lattice distortion.

Spin density

The character of the Fe $3d$ orbitals produced from a DFT+U calculation is very different from those of PBE. As a result, we expected to see a significant difference in the predicted total spin densities depending on the SPOs used in the trial wave function. An open question was the extent to which subsequent optimization of the trial wave function would correct any deficiencies. To illustrate the differences in the optimized trial wave functions, we show contours of the difference in the total spin density with respect to a SJ wave function composed of PBE SPOs in fig. 2. While both the backflow and multi-determinant trial wave functions show only small perturbations in the spin density as compared to the SJ PBE reference, the orbital optimized trial wave function yields a significantly different spin density. Evidently, the qualitatively distinct character of the spin density between PBE and PBE+U SPOs is effectively erased with orbital optimization, in concordance with the comparison of the total energy shown in fig. 1. This suggests that with orbital optimization the QMC trial wave function and its associated observables are independent of the quality of the original underlying SPO set. Further, this gives confidence that observables estimated from such a trial wave function give "right answers for the right reason".

Equilibrium Lattice Distortion

In the ground state, the nominally cubic B1 crystal structure of AFM FeO is slightly elongated along the [111] direction, thereby simultaneously increasing the inter-planar spacing and decreasing the intra-planar spacing of the iron atoms [40, 41]. This phenomenon is observed in many transition metal oxides, and is controlled by interactions between $3d$ electrons on the iron atoms[42, 43]. For that reason we expected the equilibrium lattice distortion to be very sensitive to the quality of the trial wave function. Fig. 3 shows energy versus lattice distortion at the VMC and DMC levels. The VMC results for each wave function type universally predicted lattice contraction along [111], which is qualitatively wrong as compared to experiment.

Considering the more accurate DMC calculations, we see significant improvements in both energy and predicted lattice distortion. DMC correctly shifted the predicted equilibrium lattice distortion for all trial wave functions to more positive values (extension along

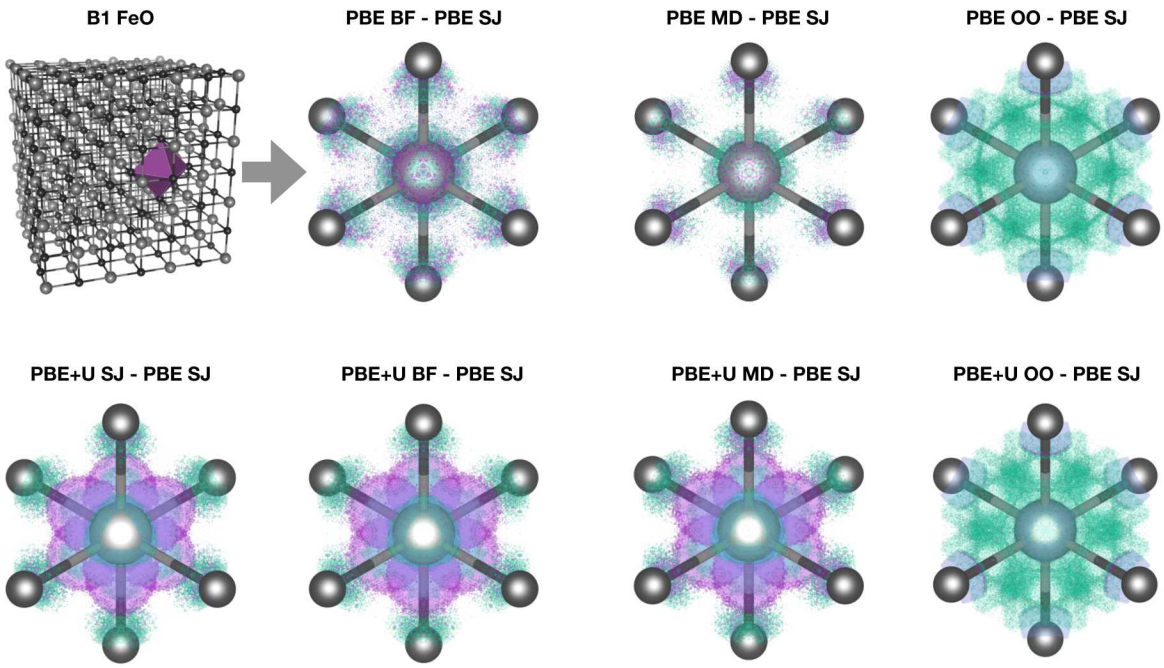

FIG. 2. (Color online) Contours of the difference in the DMC estimated total spin density between trial wave function types with respect to a single SJ trial wave function composed of PBE SPOs. Detailed views looking along [111] show a 2×10^{-9} contour interval and are restricted to a single FeO_6 octahedron for visual clarity. Iron and oxygen atoms are shown as large grey and small black spheres, respectively. green (purple) surfaces bound regions where PBE total spin density is less (greater) than that from the other SPO set.

[111]), although this shift is insufficient to recover the correct behavior in some cases. There was also a re-ordering of the relative energies of the trial wave functions as compared to VMC. Wave functions constructed from PBE+U orbitals yielded higher DMC energies as compared to those of the PBE wave functions. That the multi-determinant wave functions produce a higher energy than their single determinant counterparts at the DMC level is a reflection of the fact that wave function improvements from VMC do not necessarily guarantee a corresponding improvement with DMC. Compared to the multi-determinant expansion, the improvements in the nodal surface due to the backflow transformation and orbital optimization are readily apparent both in terms of lower total energy and lattice distortion. Indeed, the backflow and orbital optimized wave functions yielded significant energies reductions, in some cases reducing the energy by as much as 20 mHa per FeO as

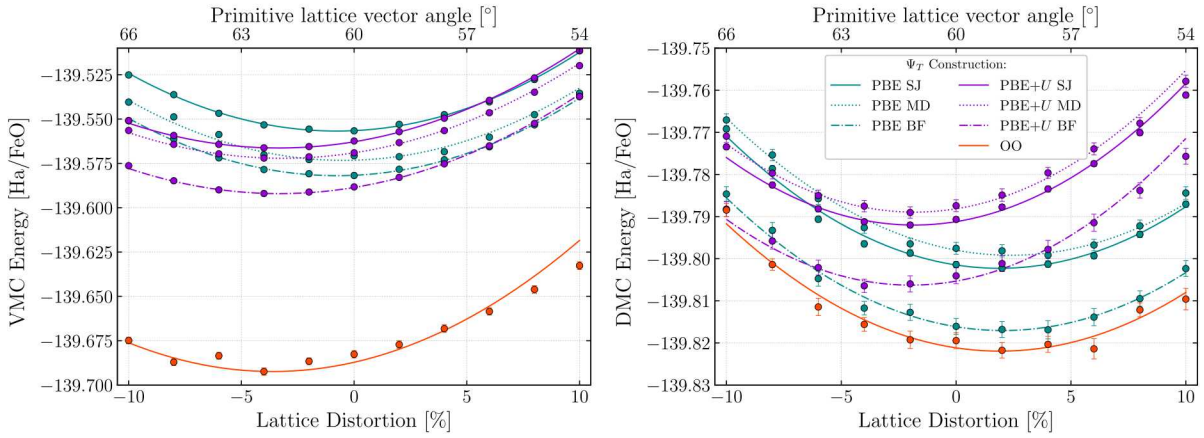

FIG. 3. (color online) Energy versus lattice distortion for VMC (left), and DMC (right) calculations with trial wave functions constructed from various DFT-based methods. The solid lines are quadratic polynomial fits to the data, and are included as a guide to the eye.

compared to the single SJ trial wave function. Overall, we found that the orbital optimized wave function produced the lowest VMC and DMC total energies, further indicating that it was more accurate.

As expected, the predicted equilibrium distortion is quite sensitive to the trial wave function. For example, a SJ trial wave function composed of PBE orbitals predicts an equilibrium distortion of about 1.9%, while the backflow and multideterminant wave functions predicted 2.0%, and 2.4%, respectively. By design, we constructed the PBE+U wave function in such a way as to accumulate excess charge between Fe atoms along [111] as compared to the other wave functions, which explains why the PBE+U wave function uniquely predicted a negative lattice distortion. Interestingly, estimates of the distortion from trial wave functions composed of PBE+U SPOs show less sensitivity, with standard SJ, backflow, and multideterminant estimates of -1.8%, -2.0%, and -1.8%, respectively. Finally, the estimated distortion from the orbital optimization wave function was 1.9%. Unfortunately, comparison to experiment is hampered by that fact that natural and synthetic FeO is non-stoichiometric. Nevertheless, experimental measurements suggest lattice distortion between about 1-2%[10, 40, 41]. Admittedly, the large uncertainty in the experimental data, likely due in part to stoichiometry, are consistent with several of our QMC estimates. However the low energy and starting point independent quality of the orbital optimization trial wave function suggest that it is the most accurate.

DISCUSSION AND CONCLUSIONS

A major goal of this study was to understand how the construction of the QMC trial wave function affected several ground state properties. The results indicate that for AFM FeO the spin density and lattice distortion were particularly sensitive to the construction of the trial wave function. The most significant result of this investigation was the demonstration of starting point independence of the QMC trial wave function with respect to the energy, spin density, and predicted lattice distortion via orbital optimization. This result suggests that wave functions of this form should provide truly *ab-initio* estimates of ground state properties of materials in which electronic correlation and many-body effects are important to account for accurately.

The results presented here are subject to several limitations. Most importantly, the 44 electron, 4 atom primitive cell considered here is too small. Currently, this limitation was necessary in order to explore advanced wave functions which scale unfavorably with system size. Here we have focused on establishing the starting point independence of a QMC trial wave function in a very challenging condensed matter system. This goal is not impeded by the use of a small cell. Future studies that seek to investigate the equation of state or other observables will need to explore the use of supercells. As for the trial wave functions, the multi-determinant expansion was very likely too small. Here we considered only single and double excitations in a small active space. Although this wave function is exponentially scaling, future studies could certainly improve upon this limitation by exploring larger active spaces and alternative methods of generating and selecting excitations [44]. Likewise for the backflow wave function, we were restricted to a single transformation. Recent advances in iterative backflow transformations may provide further improvements [45].

In conclusion, we have performed a systematic investigation of some ground state properties of AFM B1 FeO, and in particular we explored several QMC wave function generation techniques. The results suggest that the equilibrium lattice distortion and spin density are exceptionally sensitive to the construction of the trial wave function (viz. the nodal surface). We demonstrated starting point independence of the QMC trial wave function with respect to the energy, spin density, and equilibrium lattice distortion through orbital optimization. Finally, we suggest that advanced and systematically improvable QMC wave functions such as orbital optimization may soon be used more extensively in condensed matter systems for

problems where strong electronic correlation effects are important.

ACKNOWLEDGMENTS

JPT, SDP, RCC, TRM, EN, LZ, and LS were supported by the U.S. Department of Energy, Office of Science, Basic Energy Sciences, Materials Sciences and Engineering Division, as part of the Computational Materials Sciences Program and Center 263 for Predictive Simulation of Functional Materials. REC was supported by the National Science Foundation through grants TG-MCA07S016, EAR-0738061 and EAR-0530282, and by the European Research Council Advanced Grant ToMCaT and by the Carnegie Institution for Science. Sandia National Laboratories is a multimission laboratory managed and operated by National Technology & Engineering Solutions of Sandia, LLC, a wholly owned subsidiary of Honeywell International Inc., for the U.S. Department of Energy's National Nuclear Security Administration under contract DE-NA0003525. This paper describes objective technical results and analysis. Any subjective views or opinions that might be expressed in the paper do not necessarily represent the views of the U.S. Department of Energy or the United States Government.

---

* jptowns@sandia.gov

[1] D. Adler, Rev. Mod. Phys. **40**, 714 (1968).

[2] N. Mott, *Metal-Insulator Transitions* (Taylor & Francis Ltd, 1974).

[3] M. P. Pasternak, R. D. Taylor, R. Jeanloz, X. Li, J. H. Nguyen, and C. A. McCammon, Phys. Rev. Lett. **79**, 5046 (1997).

[4] J. Badro, V. Struzhkin, J. Shu, R. Hemley, H.-K. Mao, C.-C. Kao, J.-P. Rueff, and G. Shen, Phys. Rev. Lett. **83**, 4101 (1999).

[5] S. Ono, Y. Ohishi, and T. Kikegawa, Journal of Physics: Condensed Matter **19**, 036205 (2007).

[6] A. O. Shorikov, Z. V. Pchelkina, V. I. Anisimov, S. L. Skornyakov, and M. A. Korotin, Phys. Rev. B **82**, 195101 (2010).

[7] R. A. Fischer, A. J. Campbell, G. A. Shofner, O. T. Lord, P. Dera, and V. B. Prakapenka, Earth and Planetary Science Letters **304**, 496 (2011).

[8] K. Ohta, R. E. Cohen, K. Hirose, K. Haule, K. Shimizu, and Y. Ohishi, Phys. Rev. Lett. **108**, 026403 (2012).

[9] C. Shull, W. Strauser, and E. Wollan, Physical Review **83**, 333 (1951).

[10] B. T. M. Willis and H. P. Rooksby, Acta Crystallographica **6**, 827 (1953).

[11] D. G. Isaak, R. E. Cohen, M. J. Mehl, and D. J. Singh, Phys. Rev. B **47**, 7720 (1993).

[12] R. E. Cohen, I. I. Mazin, and D. G. Isaak, Science **275**, 654 (1997).

[13] I. I. Mazin, Y. Fei, R. Downs, and R. E. Cohen, American Mineralogist **83**, 451 (1998).

[14] Z. Fang, K. Terakura, H. Sawada, T. Miyazaki, and I. Solovyev, Phys. Rev. Lett. **81**, 1027 (1998).

[15] Z. Fang, I. V. Solovyev, H. Sawada, and K. Terakura, Phys. Rev. B **59**, 762 (1999).

[16] S. A. Gramsch, R. E. Cohen, and S. Y. Savrasov, American Mineralogist **88**, 257 (2003).

[17] M. Cococcioni and S. de Gironcoli, Phys. Rev. B **71**, 035105 (2005).

[18] J. c. v. Kolorenč and L. Mitas, Phys. Rev. Lett. **101**, 185502 (2008).

[19] W. M. C. Foulkes, L. Mitas, R. J. Needs, and G. Rajagopal, Rev. Mod. Phys. **73**, 33 (2001).

[20] R. Needs, M. Towler, N. Drummond, and P. L. Ríos, Journal of Physics: Condensed Matter **22**, 023201 (2010).

[21] N. D. Drummond, M. D. Towler, and R. J. Needs, Physical Review B **70**, 235119 (2004).

[22] P. López Ríos, A. Ma, N. D. Drummond, M. D. Towler, and R. J. Needs, Phys. Rev. E **74**, 066701 (2006).

[23] C. J. Umrigar, J. Toulouse, C. Filippi, S. Sorella, and R. G. Hennig, Phys. Rev. Lett. **98**, 110201 (2007).

[24] T. Helgaker, P. Jorgensen, and J. Olsen, *Molecular electronic-structure theory* (John Wiley & Sons, 2014).

[25] J. Ludovicy, K. H. Mood, and A. Lüchow, Journal of Chemical Theory and Computation **15**, 5221 (2019).

[26] J. Hermann, Z. Schätzle, and F. Noé, "Deep neural network solution of the electronic schrödinger equation," (2019), arXiv:1909.08423 [physics.comp-ph].

[27] D. Pfau, J. S. Spencer, A. G. de G. Matthews, and W. M. C. Foulkes, ArXiv **abs/1909.02487** (2019).

[28] Input files for both DFT and QMC calculations are provided in the supplementary materials.
[29] R. Jastrow, Phys. Rev. **98**, 1479 (1955).
[30] T. Kato, Communications on Pure and Applied Mathematics **10**, 151 (1957).
[31] M. G. Endres, D. B. Kaplan, J.-W. Lee, and A. N. Nicholson, Phys. Rev. Lett. **107**, 201601 (2011).
[32] P. Giannozzi, S. Baroni, N. Bonini, M. Calandra, R. Car, C. Cavazzoni, D. Ceresoli, G. L. Chiarotti, M. Cococcioni, I. Dabo, A. Dal Corso, S. de Gironcoli, S. Fabris, G. Fratesi, R. Gebauer, U. Gerstmann, C. Gougoussis, A. Kokalj, M. Lazzeri, L. Martin-Samos, N. Marzari, F. Mauri, R. Mazzarello, S. Paolini, A. Pasquarello, L. Paulatto, C. Sbraccia, S. Scandolo, G. Sclauzero, A. P. Seitsonen, A. Smogunov, P. Umari, and R. M. Wentzcovitch, Journal of Physics: Condensed Matter **21**, 395502 (2009).
[33] J. T. Krogel, J. A. Santana, and F. A. Reboredo, Physical Review B **93**, 075143 (2016).
[34] J. P. Perdew, K. Burke, and M. Ernzerhof, Phys. Rev. Lett. **77**, 3865 (1996).
[35] J. Kim, A. Baczewski, T. Beaudet, A. Benali, C. Bennett, M. Berrill, N. Blunt, E. J. L. Borda, M. Casula, D. Ceperley, S. Chiesa, bryan K clark, R. Clay, K. Delaney, M. Dewing, K. Esler, H. Hao, O. Heinonen, P. R. C. Kent, J. T. Krogel, I. Kylanpaa, Y. W. Li, M. G. Lopez, Y. Luo, F. Malone, R. Martin, A. Mathuriya, J. McMinis, C. Melton, L. Mitas, M. A. Morales, E. Neuscamman, W. Parker, S. Flores, N. A. Romero, B. Rubenstein, J. Shea, H. Shin, L. Shulenburger, A. Tillack, J. Townsend, N. Tubman, B. van der Goetz, J. Vincent, D. C. Yang, Y. Yang, S. Zhang, and L. Zhao, Journal of Physics: Condensed Matter (2018).
[36] L. Zhao and E. Neuscamman, Journal of Chemical Theory and Computation **13**, 2604 (2017).
[37] K. Esler, J. Kim, D. Ceperley, and L. Shulenburger, Computing in Science and Engineering **14**, 40 (2012).
[38] Y. Luo, K. P. Esler, P. R. C. Kent, and L. Shulenburger, The Journal of Chemical Physics **149**, 084107 (2018).
[39] M. Holzmann, B. Bernu, and D. M. Ceperley, Phys. Rev. B **74**, 104510 (2006).
[40] P. Battle and A. Cheetham, Journal of Physics C: Solid State Physics **12**, 337 (1979).
[41] H. Fjellvåg, F. Grønvold, S. Stølen, and B. Hauback, Journal of Solid State Chemistry **124**, 52 (1996).
[42] J. Kanamori, Journal of Applied Physics **31**, S14 (1960).
[43] P. W. Anderson, Phys. Rev. **79**, 350 (1950).

[44] G. H. Booth, A. Grüneis, G. Kresse, and A. Alavi, Nature **493**, 365 (2013).

[45] M. Taddei, M. Ruggeri, S. Moroni, and M. Holzmann, Phys. Rev. B **91**, 115106 (2015).